Asian Journal of Chemistry; Vol. 37, No. 9 (2025), 2274-2280
ASIAN JOURNAL OF CHEMISTRY
https://doi.org/10.14233/ajchem.2025.34166

Spectral and Biofunctional Evaluation of Aniline-*o*-Toluidine Nanostructured Copolymer: Assessing the Cytotoxicity Activity on MG-63 Cancer Cell Lines

N. CHANDRASEKARAN[1,2], D. MADHESWARI[3,*] and S. SUDARSAN[4]

[1]Department of Chemistry, Sri Vidya Mandir Arts and Science College (Autonomous), Katteri, Uthangarai, Krishnagiri-636902, India
[2]Department of Chemistry, Periyar University, Salem-636011, India
[3]Department of Chemistry, Government Arts College for Women, Salem-636008, India
[4]Department of Chemistry, Saveetha Engineering College, Thandalam, Chennai-602105, India

*Corresponding author: E-mail: drmadhu6666@yahoo.com

Received: 31 May 2025 *Accepted*: 19 August 2025 *Published online*: 30 August 2025 AJC-22109

In this work, poly(aniline-*co*-*o*-toluidine) (POT) nanostructured porous copolymer was synthesized through chemical polymerization in the presence of cationic surfactant cetyltrimethylammonium bromide (CTAB). The obtained POT copolymers were investigated by FT-IR, XRD, UV and SEM-EDX techniques. The distinct antibacterial and antifungal activities have exhibited by the as-synthesized copolymer. Various bacterial strains such as *Bacillus subtilis*, *Escherichia coli*, *Staphylococcus aureus* and *Klebsiella pneumoniae* have possess better antimicrobial efficacy than polyaniline. Furthermore, the antifungal properties of POT have exhibited greater effectiveness than those of polyaniline against *Candida albicans* and *Aspergillus niger* strains. The antioxidant capacity has measured against DPPH radicals highlighted a stronger activity in POT copolymer, with IC_{50} values of 29.4 µg/mL for polyaniline and 41.02 µg/mL for POT copolymer. Additionally, the cytotoxicity has been performed on MG-63 cancer cell lines, which indicated an IC_{50} value of 58.95 µg/mL for POT copolymer. The obtained results revealed that the development of POT based copolymer that are promising candidates for various applications, including biomedical, genetic engineering, pharmaceutical, and drug delivery fields. The obtained POT copolymer exhibited as an excellent antibacterial and anticancer activity, suggesting its potential roles in tissue engineering scaffolds, anticancer treatments, and various biomedical applications.

Keywords: Copolymer, Aniline, Surfactant, *o*-Toluidine, Cancer cell lines, Microbial activities.

INTRODUCTION

The fabrication of nanostructured conducting polymers has attracted considerable attention to the scientific communities, primarily because of their outstanding physico-chemical properties [1]. For biological systems, conducting polymers with intriguing optical and electrical properties. Polyaniline (PANI) stands out among intrinsic conducting polymers due to its notable applications in diverse industrial and biomedical fields, driven by its simple preparation, environmental stability, biocompatibility, minimal toxicity, high electrical conductivity and low cost [2-4]. However, polyaniline needs to be modified appropriately to suit the applications because of its low solubility, conductance instability and inadequate processability. To overcome these challenges, numerous tactics had developed, such as copolymerization with PANI derivatives or other polymers, doping with functionalized organic acids, creating blends and nanocomposites [5].

PANI and its nanomaterials derivatives have found an extensive use in variety of domains including materials science, biomedicine and heterogeneous catalysis [6,7]. To modify the conjugated structure, enhance processability and amalgamate the unique attributes of both homopolymers, extensive research has been carried out on the fabrication of poly(aniline-*co*-*o*-toluidine) using electrochemical and chemical oxidation methods [8,9]. This is especially significant to biological and environmental remediation applications. Diverse nanoarchitectures offer unique advantages attributed to their significant surface-to-volume ratio, resulting in improved properties of their nanocomposites. Thus, it is essential to optimize the synthesis conditions of copolymers to obtain specific morphologies and dimensions suitable for high-performance applications.

PANI material-based derivatives certainly constitute a promising sector in biomaterial science, where the combination of achievable results and ongoing technological challenges invites the need for more in-depth research and understanding. Grippingly, the cytotoxicity investigations done on fibroblast cells pectin/cadmium grafted PANI nanocomposite suggested the best toxicity effect on cells, that contributed to diffusion into biological cells and more toxicity [10]. On other hand, PANI/polypyrrole deliver striking properties for applications in biomedicine owing to their low cytotoxicity and good level of conductivity at physiological pH stemming out of organic phosphonates doping [11]. Improved biocompatibility has exhibited in PANI-taurine-based nanofibers that can also use as a bioactive conductive scaffold for tissue engineering applications [12]. Nano terpolymeric scaffold of PANI-*co*-(polydopamine-grafted-poly(D,L-lactide) can be utilized in scaffold for tissue engineering applications because of improved cell adhesion, proliferation, strong biocompatibility and biodegradability nature [13]. It is noteworthy that *o*-toluidine/chitosan co-polymer has displayed an excellent antibacterial property with exceptional capacity to terminate the bacterial cell wall as revealed by Hosseini *et al*. [14]. PANI and *o*-toluidine copolymer was successfully synthesized that examined for reactive gels unique electrochemical reaction [15]. The determination of chromium(VI) was as demonstrated through PANI/toluidine/graphene oxide modified gold electrode by electro-adsorption process [16].

Various surfactants were utilized for chemical polymerization process that could result in high surface area polymer with improved functional characteristics. The research conducted earlier advantageous of role of anionic surfactants in the synthesis of poly(aniline)-reduced graphene oxide nanocomposites, which are utilized in solar cells, resulting in an impressive power conversion efficiency of 7.60% [17]. The use of cetyltrimethylammonium bromide (CTAB) in an interfacial polymerization and self-assembly was investigated for the development of one-dimensional nanowires or nanoneedles [18]. Furthermore, the previous study [19] demonstrated that the research has focused on the status of aniline/*o*-phenylenediamine copolymerization with triton X100 as a surfactant to create supercapacitor material with exceptional functionalities such as high power density, long cycle life and speedy charge/discharge proportions.

The present investigation focuses on the fabrication of poly-(aniline-*co*-*o*-toluidine) copolymer with enhanced biocompatibility using a simple synthesis method, employing CTAB as a surfactant. The simplicity and effectiveness of this experimental technique make it particularly well suited for industrial production, significantly low costs of raw materials. To best of our knowledge, there is no much research carried out earlier on the copolymerization of *ortho*-toluidine with CTAB surfactant for biological applications.

EXPERIMENTAL

o-Toluidine, ammonium persulphate (SRL Chemicals, 95%), aniline, cetyltrimethylammonium bromide (CTAB) (Sigma-Aldrich, 98%), HCl (Nice Chemicals) and ammonium persulphate (SRL Chemicals, 95%) were used for this study. In the presence of ammonium persulphate, polyaniline-*ortho* toluidine copolymer (PoT) was developed *via* the chemical oxidative polymerization process. In briefly, 50 mL of 1 M HCl was kept ice-cold content and adequate amount of *o*-toluidine was dissolved in it. To produce a homogenous mixture, CTAB (0.002 M) was added to the monomer solution. The temperature was then kept between 0 and 5 ºC while a stipulated quantity of aniline, dissolved in 50 mL of 1 M HCl, was added. After 12 h, ammonium persulphate, five times the concentration of the monomers, was added gradually while being constantly stirred to facilitate the polymerization process. An insoluble precipitate was formed as a result. After filtering, distilled water and ethanol were used to wash this precipitate properly. The obtained product was vacuum-dried for 12 h at 70 ºC.

Characterization: Fourier transform infrared (FTIR) spectra were used to investigate the functional groups in the final product in the range of 4000-400 cm^{-1}. The spectroscopic grade KBr powder was used to produce the samples as pellets. Scanning electron microscopy (SEM) (JEOL-6360 SEM) was used to investigate the surface morphology polymers. UV-visible spectroscopy (UV-2501, Shimadzu Co., Japan) was performed across the wavelength range of 260 to 900 nm. The SEM images were obtained using a JEOL JSM 6700F electron microscope. X-ray powder diffraction spectra of samples were obtained using X-ray diffractometer (Bruker AXS D8 Advance) with Cu as a target at 1.5406 Å.

Biological studies

Antibacterial activity: The *in vitro* antibacterial activity of polymer samples was assessed against *Staphylococcus aureus*, *Klebsiella pneumoniae* (Gram +ve) and *Bacillus subtilis*, *Escherichia coli* (Gram -ve) through disc diffusion method. In a petri dish with nutrient agar, 5 different concentrations (25, 50, 75, 100 and 125 µL) of composites were placed at equal intervals on sterile Whatman filter paper with a 5 mm diameter, and a control at the center [20]. After that, the samples-containing petri dish was kept in refrigerator for 1 h at 4 ºC and then incubated for 24 h at 37 ºC. The zone of inhibition (mm) surrounding the disc against the bacterial strains was also calculated.

Antioxidant activity: A solution of DPPH$^{\bullet}$ (0.1 mM-333 µL) in methanol was mixed with 1 mL of sample dissolved in DMSO at different concentrations. After vigorous shaking, the subsequent mixture was left to equilibrate for 0.5 h at room temperature. A UV-visible spectrophotometer (model: Multiskan GO; Thermo-Fisher Scientific Inc., USA) was used to quantify the absorbance at 513 nm. Higher free radical scavenging activity is indicated by a decreased absorbance value in the reaction mixture. L-ascorbic acid (vitamin C) was used as the positive control at concentrations ranging from 10 to 500 µg/mL. The DPPH$^{\bullet}$ radical scavenging activity was calculated using eqn. 1:

$$\text{Scavenging effect (\%)} = \frac{\text{Abs}_{\text{test}} - \text{Abs}_{\text{control}}}{\text{Abs}_{\text{control}}} \times 100 \quad (1)$$

Cytocompatibility analysis: Using human osteosarcoma MG63 (HOS MG63, ATCC CRL-1427TM) cells, the biocompatibility of polymer was assessed. The cells were acquired from NCCL, Pune, India. The acquired cells were kept at 37 ºC

in a humidified environment with 5% CO_2 in Dulbecco's modified Eagle medium (DMEM, GIBCO), complemented with 10% FBS and 1% antibiotic solution. After that, the cultured cells were deposited at a density of 5×10^4 cells cm^{-2} onto the composite samples in 24-well plates. In 24-well plates, cells with same seeding density but no samples were employed as a control. Cell viability (expressed as a percentage) was compared to the control to determine cytotoxicity [20] (eqn. 2):

$$\text{Cell viability (\%)} = \frac{[\text{A}]\ \text{Test}}{[\text{A}]\ \text{Control}} \times 100 \qquad (2)$$

The initial cell adhesion study was carried out utilizing confocal microscopy with MG63 osteosarcoma cell line as a biological model. The cell cytoskeletons were dyed green (I-Fluor488) and the nuclei were stained blue (DAPI labeling). The findings of cytotoxicity test served as the basis for this investigation.

RESULTS AND DISCUSSION

FTIR studies: The microstructure of as-synthesized PANI and POT were examined through FTIR as presented in Fig. 1, the significant peaks are marked. Notably, the characteristic peaks related with PANI has appeared predominantly at 1574, 1488, 1299 and 1235 cm^{-1} [21]. The bands at 1551 and 1475 cm^{-1}, individually, classify the C=C stretching vibrations of benzenoid ring and C–N stretching vibrations of quinoid ring. The bands noticed at 1294 and 1238 cm^{-1} indicate the appearance of N–H bending vibrations and the symmetric component of C=C stretching frequency. The bands observed at 1110 cm^{-1} corresponds by the in-plane C–H bending mode, whereas the bands at 788 cm^{-1} are initiated by the out-of-plane mode. Similar, the spectral features was exhibited in POT except a minor lower wavelength shift. Thus, it is concluded from the results that both PANI and POT formation occurred successfully in the presence of CTAB surfactant.

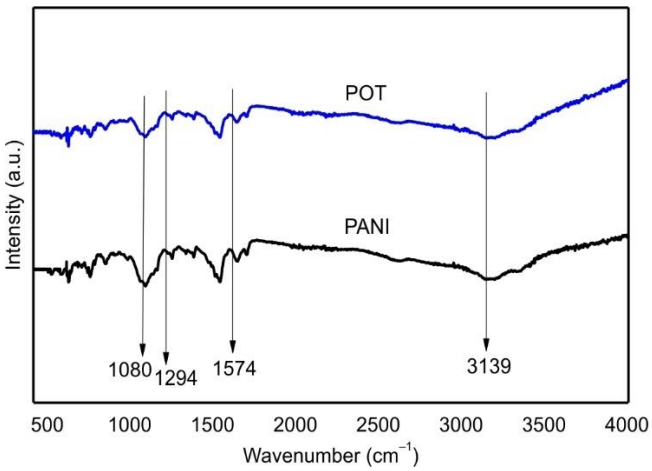

Fig. 1. FTIR spectra of PANI polymer and POT copolymer

UV-visible studies: The UV spectra of PANI and POT copolymer are shown in Fig. 2. The absorption maxima occur at 332 nm and 589 nm for PANI, whereas, the peak shifted towards 337 nm and 557 nm for POT copolymer. The observed peaks are caused by the benzenoid ring's π–π electronic transition and the quinoid rings' excitation absorption [22,23].

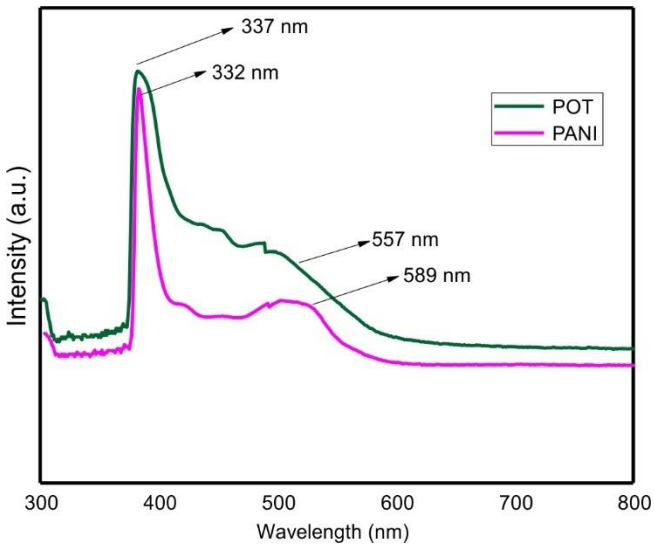

Fig. 2. UV spectral data of PANI and POT copolymer

The characteristic absorption peaks of PANI were altered in the POT spectra. The polaron transition and quinone structure related absorption intensity has diminished. These findings undoubtedly demonstrate that the copolymer production is consistent with the FTIR results.

XRD studies: The crystalline nature of synthesized PANI and POT was investigated through X-ray diffraction patterns, as shown in Fig. 3. Both the materials exhibited peaks at 2θ = 15.6º, 20.7º and 25.6º, corresponding to the (011), (020), and (200) planes. The observed positive shift associated with POT signifying little difference in the crystalline nature of PANI. Similar observations have been reported earlier also [24].

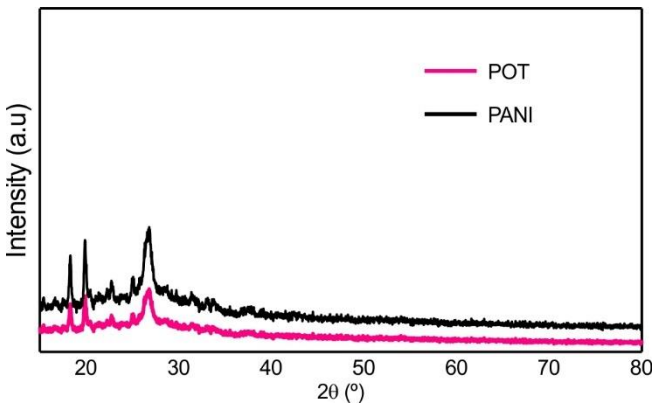

Fig. 3. X-ray diffraction studies of PANI and POT samples

SEM-EDX studies: At different magnified SEM images of POT copolymer morphologies (Fig. 4) are characterized by a tubular form alongside solid geometric characteristics, which is distinctly visible in the images. The consistent EDX spectrum and elemental mapping studies are executed as projected in Fig. 5. Furthermore, the particles are unevenly shaped, ranging from 200 to 500 nm and the aggregation of molecules is apparent in the images provided. The EDX study offers unambiguous proof of copolymer POT formation, comprising with the elemental distribution of carbon, oxygen and nitrogen as evidenced from the results of elemental mapping.

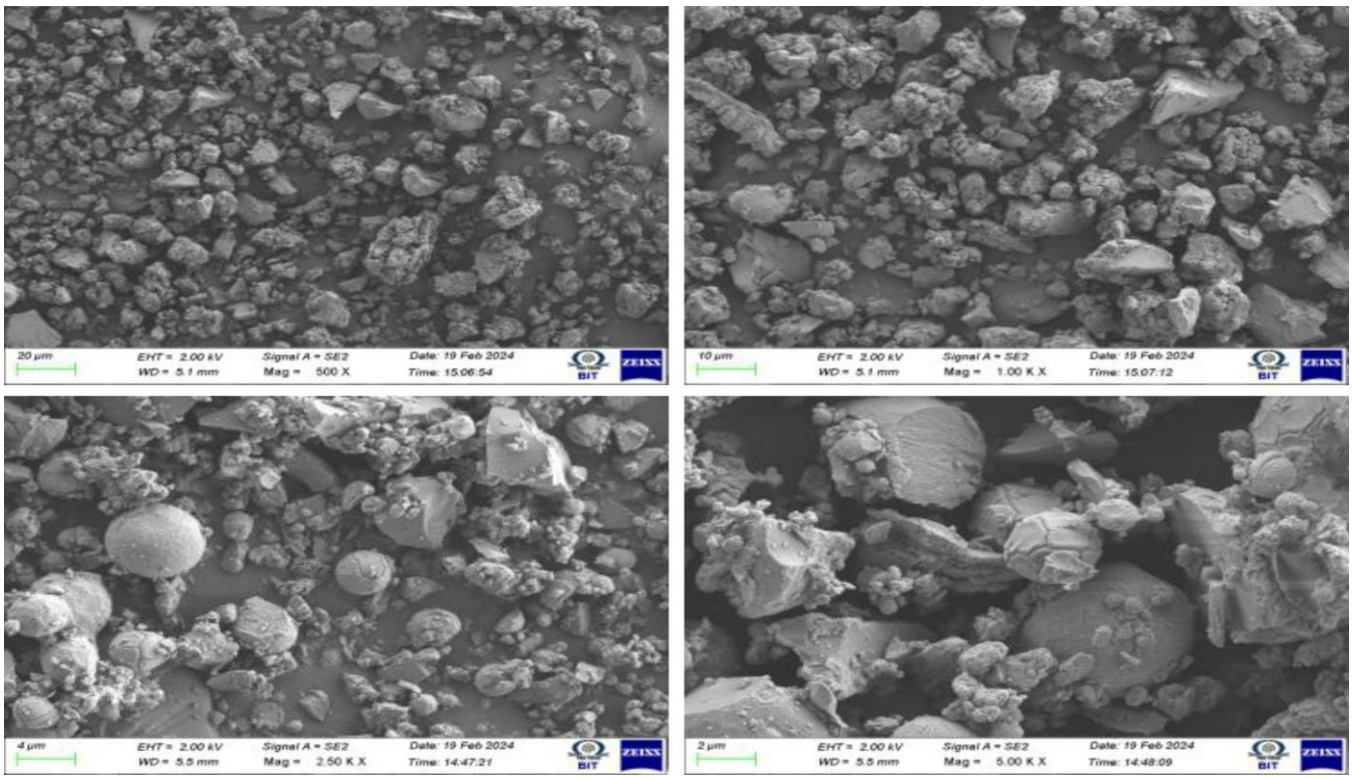

Fig. 4. SEM images POT copolymer under different magnification

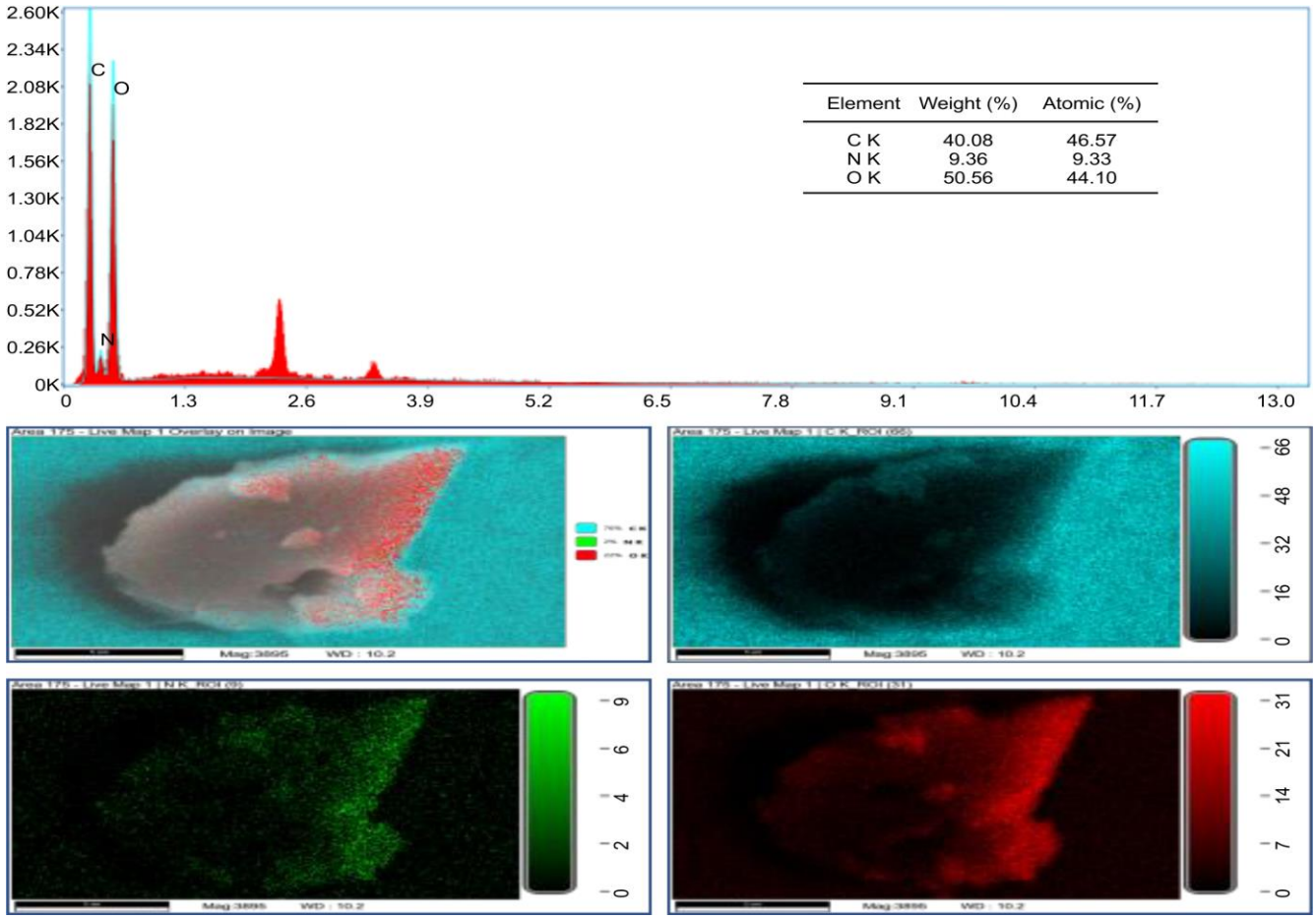

Fig. 5. EDX spectrum and elemental mapping studies of POT

Antibacterial activities: The antibacterial activity of PANI and POT has been evaluated through testing the efficiency against four different bacteria namely *Escherichia coli*, *Bacillus subtilis*, *Staphylococcus aureus*, *Klebsiella pneumoniae* at different concentrations. The results for PANI and POT are presented in Table-1, respectively. Both PANI and POT samples were appreciable activity towards inhibiting the bacterial growth. The most susceptible bacterial strains *viz*. *B. subtilis*, *E. coli* and *S. aureus*, all of which were introverted by every sample analyzed. On the other hand, *K. pneumoniae* was found to be the least susceptible among the strains tested. Also, higher the concertation, the zone of inhibition was also higher this trend was shown by both samples. At a concentration of 100 µL, the zones of inhibition observed with PANI against *B. subtilis*, *S. aureus*, *E. coli* and *K. pneumoniae* were 19 mm, 17 mm, 12 mm and 12 mm, respectively. In comparison, the POT samples exhibited slightly higher inhibition zones of 21 mm, 18 mm, 14 mm and 13 mm against the same bacterial strains. Thus, the antibacterial action was enhanced when copolymerized *o*-toluidine, which reflected by the zone of inhibition values against bacterial strains. The observed results of this study demonstrate that the incorporation of *o*-toluidine in the aniline matrix helps to boosting the activity, which could be explained by the mechanism of action involved in killing bioorganisms. It is believed that the following mechanism are involved (i) hydroxyl radical generated by polymer damages the bacterial cell walls that could lead to death of the bacteria wherein reactive oxygen species, (ii) polymer get electrostatically attached with bacterial wall disrupt the charge constitution of bacteria. From the results, we may envisage that the copolymerization of PANI with *o*-toluidine positively influenced the hydroxyl radical production as well as aids the facile attachment the polymer with the cell wall of bacteria thereby promoting the bactericidal action. Hence, the presence of *o*-toluidine played a vital role; POT exhibited an augmented activity in comparison to pristine PANI. Similar results observed when phytic acid, metal, metal oxides are incorporated in the PANI matrix [25-28].

Antifungal activities: Antifungal activities of PANI and POT were performed against *C. albicans* and *A. niger*. Based on results (Table-2), *C. albicans* was found to be the most susceptible among the tested fungal strains, while *A. niger* exhibited the least susceptibility. The PANI sample exhibited antifungal activity with zones of inhibition measuring 10 mm for *C. albicans* and 8 mm for *A. niger* at the highest tested concentration. In comparison, the POT sample showed inhibition zones of 12 mm for *A. niger* and 9 mm for *C. albicans*. These results suggest that copolymerization enhances the antifungal activity. This improvement may be attributed to the increased ability of the copolymer to penetrate fungal cells, potentially leading to cellular disruptions.

Antioxidant activities: Fig 6 presents the free radical scavenging activity of synthesized PANI and POT. The damage caused by free radicals or oxidative stress is a significant factor in the harm inflicted on the internal organs and tissues. Using ascorbic acid (vitamin C) as a reference compound, the DPPH (1,1-diphenyl-2-picrylhydrazyl) free radical scavenging assay was employed to evaluate the antioxidant activity of POT at varying concentrations (20, 40, 60, 80 and 100 µg/mL). The results indicate that scavenging activity is concentration dependent, with maximum activity observed at higher concentra-

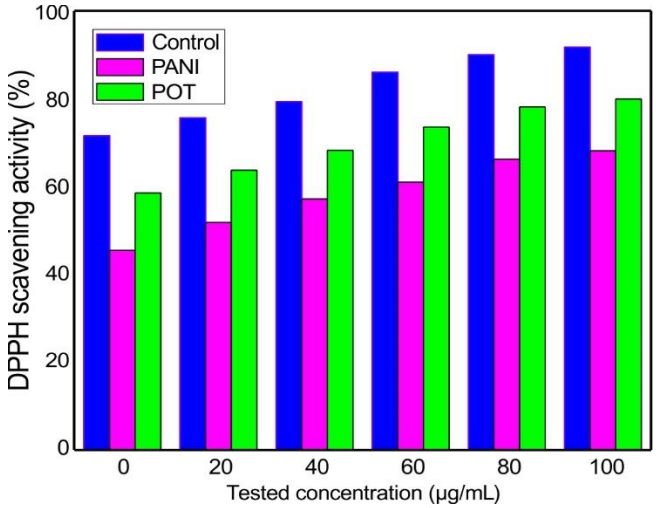

Fig. 6. DPPH radical scavenging activity of synthesized PANI and copolymer POT

TABLE-1
ANTIBACTERIAL ACTIVITY UNDER VARIED CONCENTRATION WITH PANI AND POT

Test organism	Zone of inhibition in (mm) against different concentration									
	Control		25 µL		50 µL		75 µL		100 µL	
	PANI	POT	PANI	POT	PANI	POT	PANI	POT	PANI	POT
Bacillus subtilis	25	25	14	14	16	18	17	19	19	21
Staphylococcus aureus	23	23	11	12	12	14	15	15	17	18
Escherichia coli	17	17	10	10	11	12	11	13	12	14
Klebsiella pneumoniea	21	21	9	9	9	9	11	11	12	13

TABLE-2
ANTIFUNGAL ACTIVITY OF PANI AND POT SAMPLES

Test organism	Zone of inhibition in (mm) against different concentration									
	Control		25 µL		50 µL		75 µL		100 µL	
	PANI	POT	PANI	POT	PANI	POT	PANI	POT	PANI	POT
Candida albicans	28	28	6	9	7	9	10	11	10	12
Aspergillus niger	17	17	–	–	–	–	5	6	8	9

tions. The IC_{50} values were determined to be 29.4 µg/mL for PANI and 41.02 µg/mL for POT.

Anticancer activity: The *in vitro* anticancer activity was accomplished against MCF-7 cell line by MTT test utilizing doxorubicin as standard with POT copolymer. This assay is largely contingent upon the observation. The only live cells can reduce MTT to a yellow colour, while the dead cells generally produce blue formazan products. The obtained MTT assay results reveal that as-synthesized POT copolymer is capable to hinder the growth of cancer cells as illustrated in Fig. 7. It has demonstrated an IC_{50} value of 58.95 µg/mL, as shown in Table-3.

TABLE-3
MTT ABSORPTION VALUE

Cells	MG-63				Samples nae				2C		
Blank	0	10	20	30	40	50	60	70	80	90	100
0.033	0.912	0.849	0.777	0.702	0.633	0.551	0.442	0.355	0.266	0.155	0.088
0.032	0.911	0.852	0.771	0.706	0.632	0.542	0.441	0.351	0.261	0.161	0.081
0.035	0.914	0.852	0.772	0.704	0.628	0.543	0.452	0.354	0.268	0.163	0.084
	0.912	0.851	0.773	0.704	0.631	0.545	0.445	0.353	0.265	0.160	0.084
Mean	0	7	15	23	31	40	51	61	71	82	91
Viability	100	97	85	77	69	60	49	39	29	18	9

IC_{50} = 58.95 µg/mL

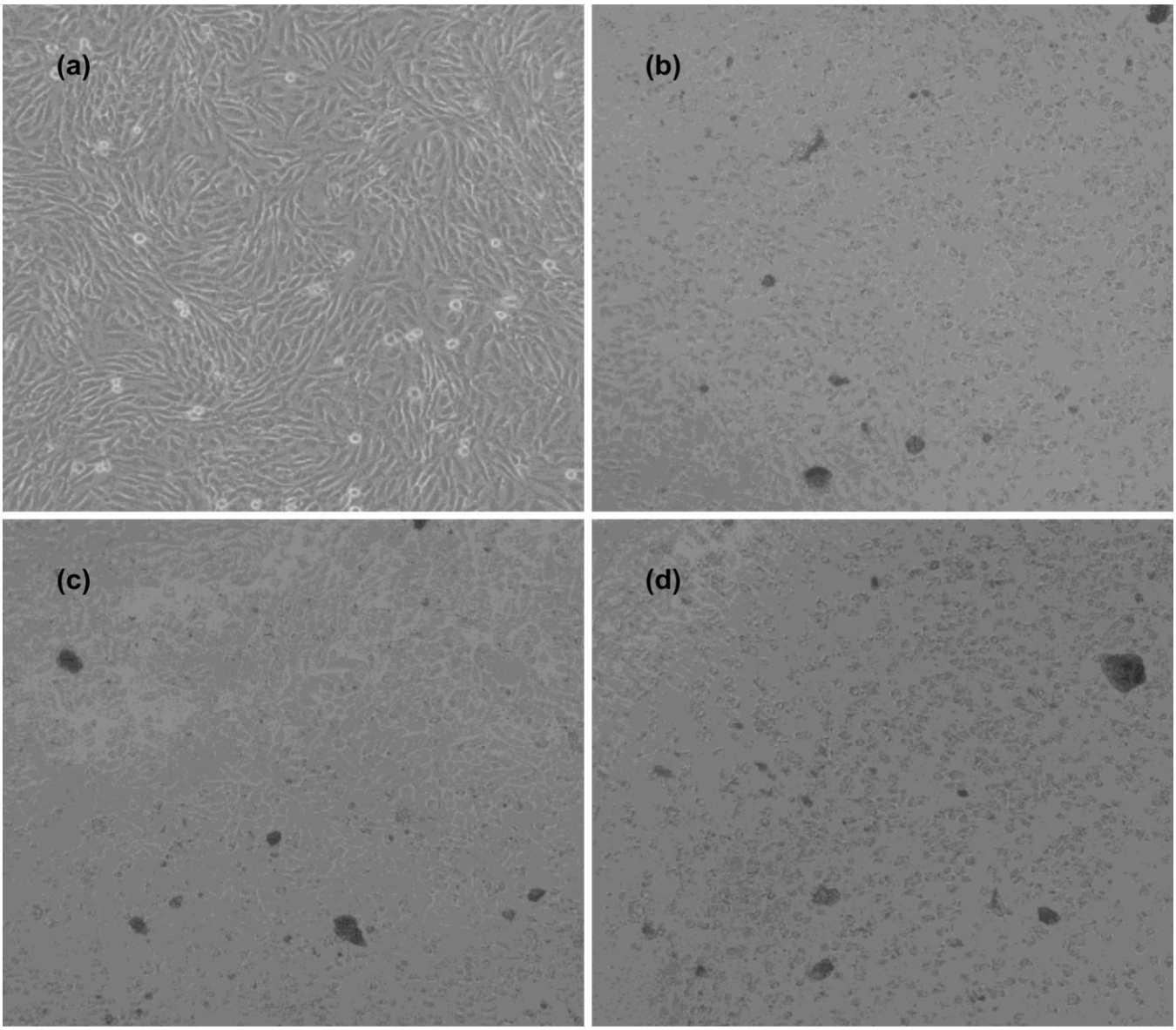

Fig. 7. MTT assay of synthesized copolymer POT tested against MG63 cell lines

Conclusion

The prominence of copolymerization in the presence of CTAB as a surfactant has been highlighted in this work and the resulting copolymer of polyaniline-*ortho*-toluidine has been biologically assessed. The UV-Vis, FT-IR, FESEM and EDX analytical techniques were used to validate the formation of polyaniline (PANI) and polyaniline-*ortho*-toluidine (POT) copolymer. The antimicrobial activity of POT was superior to that of PANI, according to the antibacterial experiments conducted with four distinct bacteria *viz*., *B. subtilis*, *E. coli*, *S. aureus* and *K. pneumoniea* at varying doses. The antifungal activity of POT was found to be higher than that of PANI when C. *albicans* and *A. niger* fungal strains. The antioxidant activity against DPPH radicals also proved higher activity with respective to IC_{50} value of 29.4 µg/mL and 41.02 µg/mL for PANI and POT samples, respectively. On this basis, the cytotoxicity activity of POT was carried out against MG-63 cancer cell lines, the study demonstrates that the IC_{50} value of 58.95 µg/mL.

ACKNOWLEDGEMENTS

The authors gratefully acknowledge the financial support provided by Sri Vidya Mandir Arts and Science College (Autonomous), Katteri, Uthangarai, Krishnagiri, India.

CONFLICT OF INTEREST

The authors declare that there is no conflict of interests regarding the publication of this article.

REFERENCES

1. B. Kalidasan, A.K. Pandey, S. Shahabuddin, M. George, K. Sharma, M. Samykano, V.V. Tyagi and R. Saidur, *Renew. Energy*, **173**, 1057 (2021); https://doi.org/10.1016/j.renene.2021.04.050
2. V. Babel and B.L. Hiran, *Polym. Compos.*, **42**, 3142 (2021); https://doi.org/10.1002/pc.26048
3. A.H. Majeed, L.A. Mohammed, O.G. Hammoodi, S. Sehgal, M.A. Alheety, K.K. Saxena, S.A. Dadoosh, I.K. Mohammed, M.M. Jasim and N.U. Salmaan, *Int. J. Polym. Sci.*, **2022**, 9047554 (2022); https://doi.org/10.1155/2022/9047554
4. R. Prabhu, T. Jeevananda, K.R. Reddy and A.V. Raghu, *Mater. Sci. Energy Technol.*, **4**, 107 (2021); https://doi.org/10.1016/j.mset.2021.02.001
5. S. Kumar, P. Kumar, R. Gupta and V. Verma, *J. Alloys Compd.*, **862**, 158331 (2021); https://doi.org/10.1016/j.jallcom.2020.158331
6. S.L. Madaswamy, S.M. Wabaidur, M.R. Khan, S.C. Lee and R. Dhanusuraman, *Macromol. Res.*, **29**, 411 (2021); https://doi.org/10.1007/s13233-021-9044-1
7. A. Emi Princess Prasanna, P. Karpagavinayagam, S. Kulandaivel and C.Vedhi, *Mater. Today Proc.*, **48**, 245 (2022); https://doi.org/10.1016/j.matpr.2020.07.076
8. M.-R. Huang, X.-G. Li, Y.-L. Yang, X.-S. Wang and D. Yan, *J. Appl. Polym. Sci.*, **81**, 1838 (2001); https://doi.org/10.1002/app.1617
9. P. Savitha and D.N. Sathyanarayana, *Polym. Int.*, **53**, 106 (2004); https://doi.org/10.1002/pi.1316
10. A. Alipour, M. Mansour Lakouraj and H. Tashakkorian, *Sci. Rep.*, **11**, 1913 (2021); https://doi.org/10.1038/s41598-020-80038-1
11. Z. Capáková, K.A. Radaszkiewicz, U. Acharya, T.H. Truong, P. Bober, J. Pacherník, V. Kašpárková, J. Stejskal, J. Pfleger, M. Lehocký and P. Humpolíček, *Mater. Sci. Eng. C*, **113**, 110986 (2020); https://doi.org/10.1016/j.msec.2020.110986
12. Z. Daraeinejad and I. Shabani, *Synth. Met.*, **271**, 116642 (2021); https://doi.org/10.1016/j.synthmet.2020.116642
13. B. Massoumi, M. Abbasian, R. Jahanban-Esfahlan, R. Mohammad-Rezaei, B. Khalilzadeh, H. Samadian, A. Rezaei, H. Derakhshankhah and M. Jaymand, *Int. J. Biol. Macromol.*, **147**, 1174 (2020); https://doi.org/10.1016/j.ijbiomac.2019.10.086
14. S. Sadat Hosseini, S.H. Hosseini and A. Hajizade, *Heliyon*, **10**, e33960 (2024); https://doi.org/10.1016/j.heliyon.2024.e33960
15. L. Rajan, M.P. Sidheekha, A. Shabeeba, S.C. Unnikrishnan and Y.A. Ismail, *Res. Chem. Intermed.*, **48**, 4313 (2022); https://doi.org/10.1007/s11164-022-04814-6
16. M.A. Hussein, A.A. Ganash and S.A. Alqarni, *Polymer-Plast. Technol. Mater.*, **58**, 1423 (2019); https://doi.org/10.1080/25740881.2018.1563121
17. E. Shanmugasundaram, V. Ganesan, V. Narayanan, M. Perumalsamy, S.V. Kuppu, P.K. Guruviah and S. Thambusamy, *Chem. Phys. Lett.*, **771**, 138517 (2021); https://doi.org/10.1016/j.cplett.2021.138517
18. J. Li, Q. Jia, J. Zhu and M. Zheng, *Polym. Int.*, **57**, 337 (2008); https://doi.org/10.1002/pi.2353
19. N. Chandrasekaran, D. Madheswari and S. Sudarsan, *Ionics*, **30**, 5755 (2024); https://doi.org/10.1007/s11581-024-05693-0
20. H.-L. Qin, Z.-W. Zhang, L. Ravindar and K.P. Rakesh, *Eur. J. Med. Chem.*, **207**, 112832 (2020); https://doi.org/10.1016/j.ejmech.2020.112832
21. A. Yadav, N. Mohammad and P.K. Khanna, *Mater. Adv.*, **4**, 4409 (2023); https://doi.org/10.1039/D3MA00394A
22. J. Tong, W. Pan, J. Ma, J. Luo and R. Liu, *Prog. Org. Coat.*, **175**, 107366 (2023); https://doi.org/10.1016/j.porgcoat.2022.107366
23. A. Singh, P. Chauhan, A. Verma and B.C. Yadav, *Adv. Compos. Hybrid Mater.*, **7**, 88 (2024); https://doi.org/10.1007/s42114-024-00878-7
24. B.T. Vijaykumar, B. Manjunatha and B. Sannakki, *Indian J. Sci. Technol.*, **17**, 3361 (2024); https://doi.org/10.17485/IJST/v17i32.334
25. J. Jesbin Jebarshia, T. Preethi, S. Ashokan, N. Geetha and K. Senthil, *Inorg. Chem. Commun.*, **16**, 111971 (2024); https://doi.org/10.1016/j.inoche.2023.111971
26. D. Switha, S.K. Basha and V.S. Kumari, *Polym. Bull.*, **80**, 11439 (2023); https://doi.org/10.1007/s00289-022-04616-1
27. A. Nafady, A.A. Alothman and S.F. Shaikh, *Int. J. Biol. Macromol.*, **244**, 125384 (2023); https://doi.org/10.1016/j.ijbiomac.2023.125384
28. B.A. Shah, A. Sardar, W. Peng, S.T.U. Din, S. Hamayoun, S. Li and B. Yuan, *Inorg. Chem. Front.*, **10**, 6339 (2023); https://doi.org/10.1039/D3QI01316B